Sexually Dimorphic Diet-Induced Insulin Resistance in Obese Tissue Inhibitor of Metalloproteinase-2 (TIMP-2)-Deficient Mice

Diane M. Jaworski, Olga Sideleva, Holly M. Stradecki, Garret D. Langlois, Aida Habibovic, Basanthi Satish, William G. Tharp, James Lausier, Kyla LaRock, Thomas L. Jetton, Mina Peshavaria, and Richard E. Pratley

Department of Anatomy and Neurobiology (D.M.J., H.M.S., G.D.L.), University of Vermont College of Medicine, Burlington, Vermont 05405; and Department of Medicine (O.S., A.H., B.S., W.G.T., J.L., K.L., T.L.J., M.P., R.E.P.), Division of Endocrinology, Diabetes and Metabolism, Colchester Research Facility, University of Vermont College of Medicine, Colchester, Vermont 05446

Circulating levels of matrix metalloproteinases (MMPs) and their endogenous inhibitors, tissue inhibitor of metalloproteinases (TIMPs), are altered in human obesity and may contribute to its pathology. TIMP-2 exerts MMP-dependent (MMP inhibition and pro-MMP-2 activation) and MMP-independent functions. To assess the role of TIMP-2 in a murine model of nutritionally induced obesity, weight gain in wild-type and TIMP-2 deficient [knockout (KO)] mice fed a chow or high-fat diet (HFD) was determined. The effects of diet on glucose tolerance and insulin sensitivity, as well as pancreatic β-cell and adipocyte physiology, were assessed. Chow-fed TIMP-2 KO mice of both sexes became obese but maintained relatively normal glucose tolerance and insulin sensitivity. Obesity was exacerbated on the HFD. However, HFD-fed male, but not female, TIMP-2 KO mice developed insulin resistance with reduced glucose transporter 2 and pancreatic and duodenal homeobox 1 levels, despite increased β-cell mass and hyperplasia. Thus, although β-cell mass was increased, HFD-fed male TIMP-2 KO mice develop diabetes likely due to β-cell exhaustion and failure. TIMP-2 mRNA, whose expression was greatest in sc adipose tissue, was down-regulated in HFD-fed wild-type males, but not females. Furthermore, HFD increased membrane type 1-MMP (MMP-14) expression and activity in male, but not female, sc adipose tissue. Strikingly, MMP-14 expression increased to a greater extent in TIMP-2 KO males and was associated with decreased adipocyte collagen. Taken together, these findings demonstrate a role for TIMP-2 in maintaining extracellular matrix integrity necessary for normal β-cell and adipocyte physiology and that loss of extracellular matrix integrity may underlie diabetic and obesogenic phenotypes. **(*Endocrinology* 152: 1300–1313, 2011)**

Obesity has reached epidemic proportions in the United States. In 2007–2008, 68% of adults and 10% of children were overweight or obese (body mass index $\geq$ 25) (1, 2). Although the rate of obesity increase appears to be slowing, type 2 diabetes mellitus (T2DM) incidence continues to increase, particularly among children and adults 60 yr and older (Centers for Disease Control and Prevention 2007 National Diabetes Fact Sheet). Although obesity increases the risk for T2DM, many obese individuals are able to maintain normal glucose tolerance, because pancreatic β-cells compensate appropriately for the degree of insulin resistance.

Differences in the distribution of adipose stores, and not the overall level of obesity *per se*, appear key contributors to T2DM development. Although it is well accepted that insulin resistance and T2DM are more strongly as-

ISSN Print 0013-7227 ISSN Online 1945-7170
Printed in U.S.A.

doi: 10.1210/en.2010-1029 Received September 3, 2010. Accepted December 23, 2010.
First Published Online February 1, 2011

Abbreviations: EMR1, Epidermal growth factor module-containing mucin-like hormone receptor 1; ECM, extracellular matrix; GLUT2, glucose transporter 2; HFD, high-fat diet; IPGTT, ip glucose tolerance test; IPITT, ip insulin tolerance test; KO, knockout; MCP-1, monocyte chemotactic protein 1; MMP, matrix metalloproteinase; MT1, membrane type 1; Pdx1, pancreatic and duodenal homeobox 1; PECAM-1, platelet/endothelial cell adhesion molecule 1; T2DM, type 2 diabetes mellitus; TIMP, tissue inhibitor of metalloproteinase; WT, wild type.

sociated with visceral than sc adiposity (3), recent studies suggest an even stronger correlation with fat deposition in ectopic sites (*e.g.* hepatosteatosis and myosteatosis) (4, 5). The factors leading to ectopic fat deposition remain largely unknown. Perhaps the production of soluble signaling molecules from distinct adipose depots could link differential adipogenesis and T2DM.

Matrix metalloproteinases (MMPs) are a family of zinc-dependent proteinases that regulate tissue integrity via extracellular matrix (ECM) degradation and signal transduction via "shedding" of cell surface receptors but also promote differentiation via the release of sequestered growth factors (6). The need to characterize the adipose protease profile has been clearly demonstrated in MMP-deficient mice subjected to a high-fat diet (HFD). MMP-3, MMP-11, and MMP-19 knockout (KO) mice display a hyperlipotrophic phenotype (7–9). In contrast, MMP-2 and MMP-14 KO adipose tissue is lipodystrophic (10–13). MMP-9 and MMP-10 do not significantly contribute to murine adipose tissue development (14, 15), even though plasma MMP-9 is increased in obese humans (16).

The four tissue inhibitor of metalloproteinases (TIMPs) not only regulate MMP activity (*e.g.* MMP inhibition and pro-MMP activation) (17) but also exert diverse MMP-independent functions (*e.g.* cell cycle arrest and antiangiogenesis) (18). Although male HFD-fed TIMP-1 KO mice are protected from obesity (19), female chow-fed TIMP-1 KO mice are obese (20). The basis for this sexual dimorphism is, at present, unknown. TIMP-3 KO mice only displayed HFD-induced diabetes in conjunction with insulin receptor haploinsufficiency (21). The metabolic status of TIMP-4 KO mice is unknown.

Here, we show that TIMP-2 KO mice of both sexes become obese even when fed a standard chow diet. Obesity is exacerbated on a HFD and is associated with increased adipocyte cell size, a redistribution of adipose stores, and increased adipokine expression. Although chow-fed KO mice are obese, they have normal glucose tolerance and insulin sensitivity. In contrast, male, but not female, HFD-fed TIMP-2 KO mice are insulin resistant and, in spite of enhanced β-cell hyperplasia, become hyperglycemic, probably due to β-cell exhaustion and failure. Taken together, our results model diet-induced human obesity in that TIMP-2 KO mice are spared the metabolic consequences of obesity unless they consume an unhealthy fat-laden diet.

Materials and Methods

Animals

All procedures were in accordance with approved University of Vermont Animal Care and Use Committee protocols. TIMP-2 KO mice (22) (after 10 back-crosses with Charles Rivers' C57Bl/6 mice) and wild-type (WT) controls were maintained as congenic homozygous breeders. At 2 months of age, littermates were singly housed and either remained on the standard chow diet (ProLab RMH 3000, 4.1 kcal/g with 26% protein, 60% carbohydrate, 14% fat; Purina LabDiet, Scotts Distributing Inc., Hudson, NH) or switched to a HFD (5.24 kcal/g with 20% protein; 20% carbohydrate; and 60% fat, which is 37.1% saturated, 46.0% monounsaturated, and 16.9% polyunsaturated; Research Diets, Inc., New Brunswick, NJ) for 3 months. In both cases, mice had *ad libitum* access to food and water. Food consumption and animal weight were measured daily within 1 h of the light (sleep) cycle. At the termination of the study, the mice were humanely killed via exsanguination, tissues were rapidly removed and frozen at −80 C for quantitative real-time PCR and Western blot analyses or immersion fixed for immunohistochemical analysis.

Serological testing

Fed glucose and plasma insulin levels were monitored from a small nick in the tail vein at 1000 h. Fasting commenced at 1800 h at the beginning of the dark (feeding) cycle, the next day mice were weighed, and their fasting blood glucose and insulin levels were monitored at 1000 h. The mice were injected with 2 g/kg body weight of glucose [ip glucose tolerance test (IPGTT)] or 0.75 mU/kg of human insulin (Eli Lilly) [ip insulin tolerance test (IPITT)] in sterile saline after 55 and 78 d, respectively. Blood glucose values were monitored using a standard glucometer (LifeScan One Touch Ultra, Milpitas, CA) at 0, 5, 15, 30, 60, 90, and 120 min after injection. To monitor insulin levels, plasma was collected 0, 30, and 120 min after glucose injection.

Insulin and leptin enzyme immunoassay

Plasma insulin and leptin levels were determined by enzyme immunoassay according to manufacturer's instructions (Alpco Diagnostics, Salem, NH). Optical density readings were converted to ng/ml or pg/ml, respectively, using kit provided standards and Prism software (GraphPad, San Diego, CA). Correlation of leptin concentration to body weight was determined using Microsoft Excel.

β-Cell morphometry

β-Cell mass and proliferation were determined as described (23). For β-cell mass, 5-μm-thick paraffin sections were immunostained with guinea pig antiinsulin primary antibody (1:1000, AB3340; Millipore, Billerica, MA). Only islets more than five-cell diameters were included for islet β-cell surface area measurements. The proportion of islet β-cell surface area *vs.* whole pancreas surface area was determined planimetrically by digital imaging. β-Cell mass was determined by multiplying the average β-cell surface area per animal by their pancreatic weight. The relative size frequency of β-cell clusters, categorized into one of six classes, was analyzed with National Institutes of Health ImageJ using the same sections used for β-cell mass measurements. For β-cell proliferation, 5-μm-thick paraffin sections were immunostained with mouse antihuman Ki-67 (1:500, no. 610968; BD Biosciences, San Jose, CA), then biotin-conjugated donkey antimouse (Jackson ImmunoResearch, West Grove, PA), and incubation with streptavidin-horseradish peroxidase (1:300; Zymed, San Francisco, CA). After development with 3,3'-diaminobenzidine tetrahydrochloride/H_2O_2, sections were immunostained for insulin, as described above, and finally counter-

stained with hematoxylin. The number of Ki-67-positive nuclei per 1000–1500 islet β-cells was counted for each animal.

Islet isolation

Pancreatic islets were isolated by collagenase digestion, separated by histopaque density gradient centrifugation, and hand picked under a stereomicroscope as described (24).

Western blot analysis

Western blot analysis was performed as previously described (25). Protein expression in isolated islets was determined using rabbit antihuman TIMP-2 (1:1500, AB801; Millipore), rabbit antirat glucose transporter 2 (GLUT2) (1:1000, no. 07-1402; Millipore), mouse antirat pancreatic and duodenal homeobox 1 (Pdx1) (1:1000, Developmental Studies Hybridoma Bank clone F6A11), and normalization to mouse antirat β-tubulin (1:2000, T4026; Sigma, St. Louis, MO). Protein expression in sc adipose tissue was first assessed using rabbit antihuman MMP-14 (1:2500, Ab38971; Abcam, Cambridge, MA). Immunocomplexes were visualized by enhanced chemiluminescence (PerkinElmer Life Sciences, Boston, MA), stripped from the membrane by incubation with Restore Plus Western Blot Stripping buffer (Pierce, Rockford, IL) and stripping solution [0.2 M glycine and 0.5 M NaCl (pH 2.5)] for 10 min each followed by 15-min washes in Tris-buffered saline and Tris-buffered saline with Tween 20. Blots were then incubated with goat antimouse CD31/platelet/endothelial cell adhesion molecule 1 (PECAM-1) (1:250; sc-1506; Santa Cruz Biotechnology, Inc., Santa Cruz, CA) and immunocomplexes detected as before. Finally, after stripping as above, blots were reprobed with goat antihuman actin (1:1000, sc-1616; Santa Cruz Biotechnology, Inc.). Densitometry was performed using Quantity One software (Bio-Rad, Hercules, CA).

Microscopy

Confocal immunofluorescence imaging with guinea pig antiglucagon (1:1000, no. 4031-01F; Millipore), rabbit antirat GLUT2 (1:1000, no. 07-1402; Millipore), mouse antirat Pdx1 (1:1000, Developmental Studies Hybridoma Bank clone F6A11), rabbit antihuman TIMP-2 (1:200, no. 9013-2609; Biogenesis, Kingston, NH), rat antimouse Mac-2 (1:250; Cedarlane Laboratories Ltd, Hornby, Ontario, CA), and rabbit antihuman MMP-14 (1:500, Ab38971; Abcam) was performed as described (23).

Adipose tissue morphology was revealed by hematoxylin and eosin staining using standard histological techniques. Differential collagen staining was revealed by Sirius Red staining and polarization microscopy (26).

Adipose weight and adipocyte size determination

Four main fat depots with known discrete anatomical locations were collected: 1) posterior sc depot, located at the base of the hind legs, indicated as sc; 2) perigonadal depots, enveloped and bound to the epididymis by the peritoneal leaflets in males or surrounding ovaries, uterus, and bladder in females, indicated as epi or gonad; 3) three visceral fat depots located in the abdominal cavities, including ip, mesenteric, and omental fat, combined as visceral fat, indicated as visc; and 4) brown adipose tissue from the interscapular area, indicated as brown. Tissues were weighed and snap frozen in liquid nitrogen for RNA and protein extractions.

Adipocyte size was determined on 8-μm-thick hematoxylin stained sections. Between 150 and 1000 adipocyte diameters were measured in 8–10 random high-power fields from at least two noncontiguous tissue sections per sample using MetaMorph software (Molecular Devices, Sunnyvale, CA).

Quantitative real-time PCR

Total RNA from adipose tissue was extracted using an RNeasy Mini kit (QIAGEN, Valencia, CA) and cDNA synthesized using the Advantage RT for PCR kit (CLONTECH; Palo Alto, CA) following manufacturer's instructions. Quantitative real-time PCR with cDNA corresponding to 20 ng total RNA, 10 μl of 2× TaqMan Universal PCR Master Mix, and 1 μl of TaqMan assay in a 20 μl reaction volume was performed on a 7300 Real-Time PCR System (Applied Biosystems, Foster City, CA) using standard cycling conditions. Relative gene expression was determined using standard curves. TaqMan Gene Expression Assays (Applied Biosystems) were used to measure the transcription levels of TIMP-2 (Mm00441825_m1), adiponectin (Mm01343606_m1), leptin (Mm00434759_m1), epidermal growth factor module-containing mucin-like hormone receptor 1 (EMR1) (Mm00802530_m1), monocyte chemotactic protein 1 (MCP-1) (Mm00441242_m1), IL-6 (Mm00446191_m1), and TNFα (Mm00443258_m1). Gene expression was normalized to hypoxanthine-guanine phosphoribosyltransferase 1 (Mm01545399_m1).

Statistical analysis

Data are presented as mean ± SEM. Significant interactions were identified by two-way ANOVA with Bonferroni's multiple comparison tests or unpaired Student's t test using Prism software (GraphPad). Statistical significance was assigned at probability of $P < 0.05$.

Results

TIMP-2 KO mice become obese independent of diet composition

TIMP-2 KO mice develop age-dependent obesity. At postnatal d 21, TIMP-2 KO mice of both sexes had weights comparable with WT mice. However, by 3 months of age, TIMP-2 KO mice exhibited significantly greater body weights than WT mice, and weight continued to increase unabated to 1 yr of age (Jaworski, D. M., unpublished observation). Because mice were maintained as homozygous breeders and perturbations in maternal nutritional status (*e.g.* undernutrition, obesity, and diabetes) can irreversibly alter structures responsible for the control of ingestive behavior and energy expenditure (27), weight gain in offspring from heterozygous pairings was determined. Even with the small sample size (n = 3), due to reduced frequency of sex-matched WT and TIMP-2 KO littermates, TIMP-2 KO mice weighed more than their WT littermates at 3 months of age (M: WT, 25.45 ± 0.33 g; KO, 29.50 ± 0.69 g; $P = 0.006$; and F: WT, 19.14 ± 0.25 g; KO, 23.01 ± 0.37 g; $P = 0.001$), suggesting that altered gestational metabolic programming is not the basis for TIMP-2 KO obesity. Thus, studies were

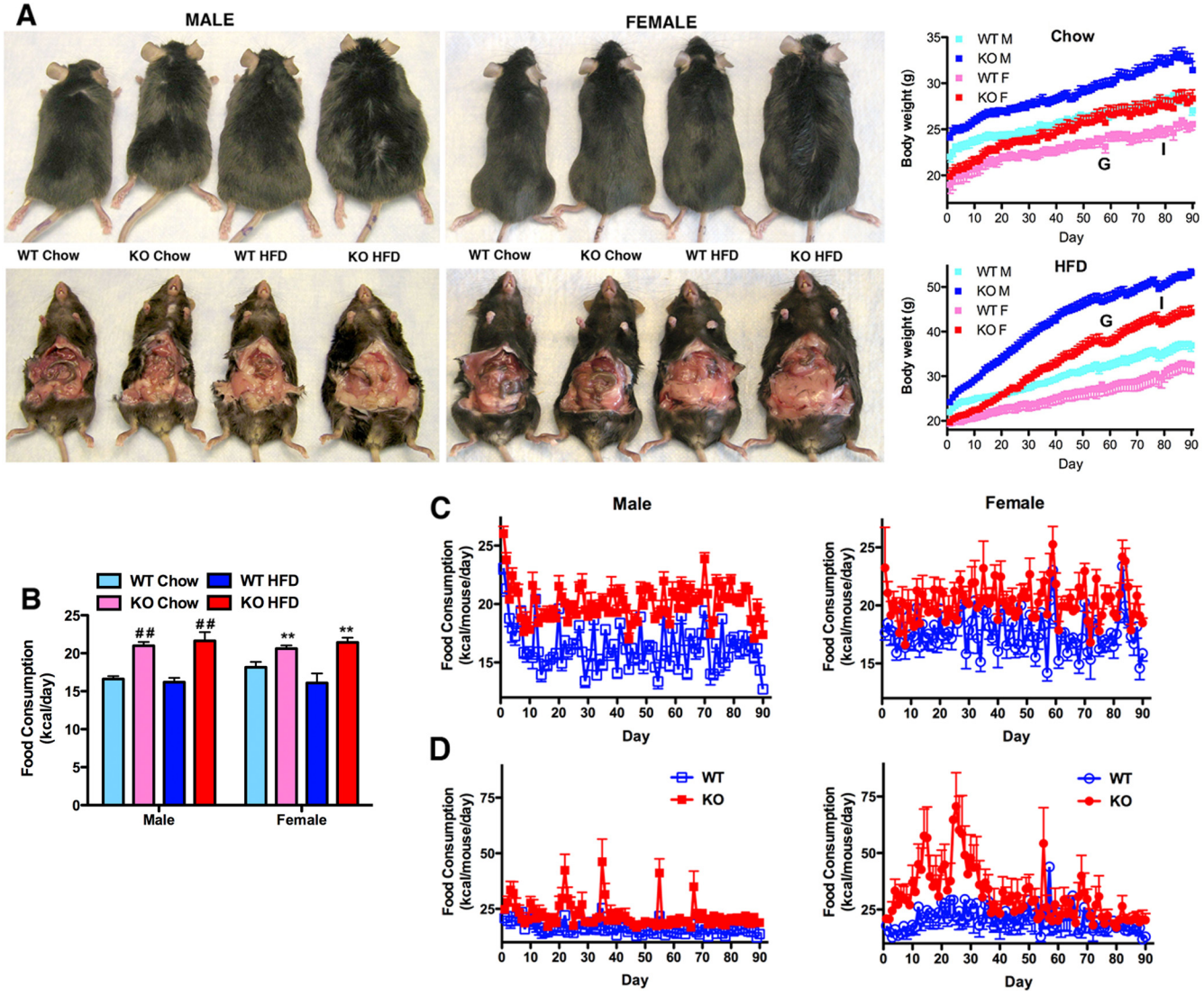

FIG. 1. Obesity and hyperphagia in TIMP-2 KO mice. A, Regardless of diet type, TIMP-2 KO mice weighed significantly more than WT mice. Weight loss corresponds to IPGTT (G) and IPITT (I). B, Average daily food consumption over the 3-month study revealed that TIMP-2 KO mice were hyperphagic (M, $P < 0.0001$; F, $P = 0.01$). C, Chow-fed male TIMP-2 KO mice were more hyperphagic than female TIMP-2 KO mice. The decline in food consumption after d 80 was not due to obesity-induced autoregulation of feeding but a response to overnight starvation for ITT (see weight loss in A). D, HFD consumption in male TIMP-2 KO mice significantly spiked after complete cage change but not replacing bedding alone. HFD-fed female TIMP-2 KO mice showed dramatically increased food consumption initially but remained hyperphagic throughout the diet and also had increased food intake upon cage change. n = 8; **, $P \leq 0.01$; ##, $P < 0.0001$.

undertaken to determine the basis for excessive weight gain in the absence of TIMP-2.

To determine the effect of diet on TIMP-2 KO obesity, 8-wk-old (*i.e.* before the onset of TIMP-2 KO obesity; M: WT, 22.48 ± 0.84 g; KO, 24.02 ± 0.38 g; $P = 0.13$; and F: WT, 18.75 ± 0.74 g; KO, 19.91 ± 0.48 g; $P = 0.21$) WT and TIMP-2 KO mice were either maintained on a standard chow diet (*i.e.* 4.1 kcal/g) or switched to a HFD containing 60% fat (*i.e.* 5.24 kcal/g), and their body weights were monitored daily for 3 months (Fig. 1A). Corroborating our previous observations, chow-fed TIMP-2 KO mice of both sexes gained more weight than WT mice over the 3-month study, and female TIMP-2 KO mice weighed as much as male WT mice at the study termination. Weight gain was exacerbated in HFD-fed TIMP-2 KO mice and was associated with greater adiposity (Fig. 1A and also see Fig. 5B). TIMP-2 KO mice maintained on the HFD for 5 months (*e.g.* ~60 g male weight) failed to show plateau of weight gain (data not shown), suggesting a defect in central recognition of and compensation to adequate energy stores.

A parsimonious explanation for TIMP-2 KO mouse obesity is a failure to regulate caloric intake; thus, food consumption was measured (Fig. 1, B–D). To most accurately assess food intake, mice need to be individually housed (Fig. 1, B–D). Because social isolation is a stressor, the mean chow consumption of group housed mice was monitored daily for 5 d before individual housing. TIMP-2 KO mice of both sexes were hyperphagic (*i.e.* 8.37 kcal/d excess in males and 3.36

kcal/d excess in females) even before obesity onset. Two-way ANOVA revealed that regardless of diet, mean food consumption of individually housed TIMP-2 KO mice of both sexes was significantly greater than similarly housed WT mice over the 3-month study (Fig. 1B). Hyperphagia was more pronounced in chow-fed male than female TIMP-2 KO mice (Fig. 1C). HFD-fed WT mice of both sexes showed little daily variability in food intake (Fig. 1D). In contrast, HFD-fed TIMP-2 KO mice displayed dramatic increase in food intake upon cage change (males) or upon individual housing (females) (Fig. 1D). Taken together, our data demonstrate that, regardless of diet, TIMP-2 KO mice were hyperphagic and did not adjust caloric intake concomitant with increased adiposity or consumption of an energy-rich diet.

Sexually dimorphic insulin resistance in TIMP-2 KO mice

To assess the physiological effects of TIMP-2 KO obesity, plasma glucose, insulin, and leptin levels were measured at the study start and termination (Fig. 2). Although a significant sex effect was present at the study start (*i.e.* decreased fed and fasting glucose and increased insulin and leptin levels in female mice; $P = 0.02$, $P = 0.039$, $P = 0.0005$, and $P < 0.0001$, respectively), no genotype effect was present, suggesting that TIMP-2 KO mice were not overtly diabetic (Fig. 2A). Furthermore, although TIMP-2 KO mice were hyperphagic at the study start, this was not due to reduced leptin levels. Similar results were obtained in chow-fed mice at the study termination (Fig. 2B). Therefore, although chow-fed TIMP-2 KO mice were obese, they did not exhibit diabetes. In contrast, HFD-fed TIMP-2 KO mice at the study termination were hyperglycemic, hyperinsulinemic, and hyperleptinemic (Fig. 2C). Although hyperleptinemic, the strong correlation (M, $R^2 = 0.85$ and F, $R^2 = 0.89$) with body weight suggests that the increased plasma leptin in TIMP-2 KO mice is proportionate to their greater adiposity (see Fig. 5B). Similar results were obtained when normalized to net adipose weight. Inasmuch as chow-fed TIMP-2 KO mice appear to be protected from the adverse metabolic consequences of their obesity, diet quality, and not obesity *per se*, is a key factor in the development of their diabetes.

To further characterize altered energy homeostasis in HFD-fed TIMP-2 KO mice, we next measured glucose tolerance and insulin sensitivity by IPGTT and IPITT, re-

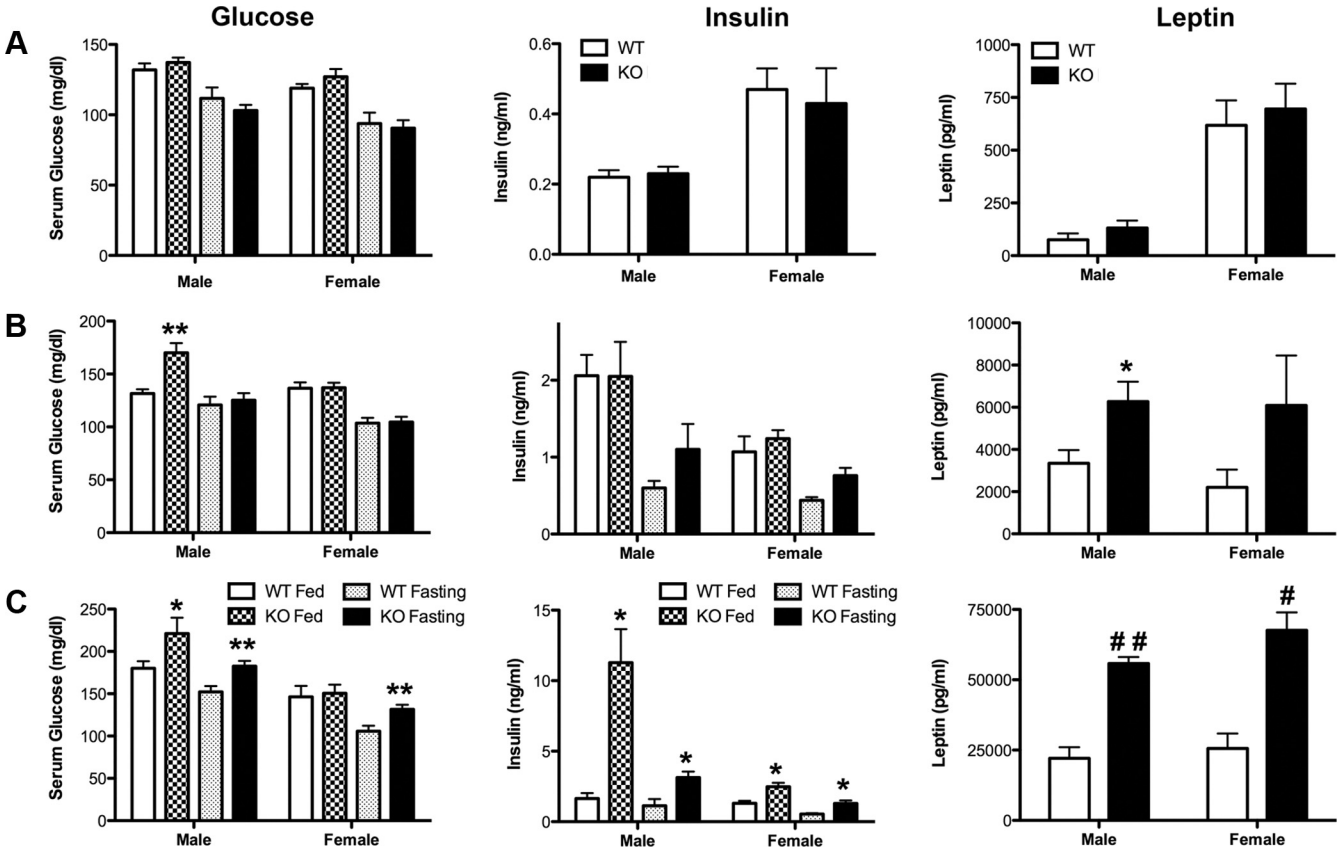

FIG. 2. Diet-induced metabolic dysfunction in TIMP-2 KO mice. A, At the study start, plasma glucose, insulin, and leptin levels were comparable in WT and TIMP-2 KO mice, suggesting that KO mice were not overtly diabetic and TIMP-2 KO hyperphagia was not due to reduced leptin. B, At the study termination, even though chow-fed TIMP-2 KO mice weighed considerably more than WT mice, plasma glucose, insulin, and leptin levels were comparable. C, In contrast, HFD-fed TIMP-2 KO mice of both sexes were hyperglycemic, hyperinsulinemic, and hyperleptinemic at the study termination. n = 4–8 per sex, genotype, and diet. *, $P < 0.05$; **, $P \leq 0.01$; #, $P \leq 0.001$; ##, $P < 0.0001$.

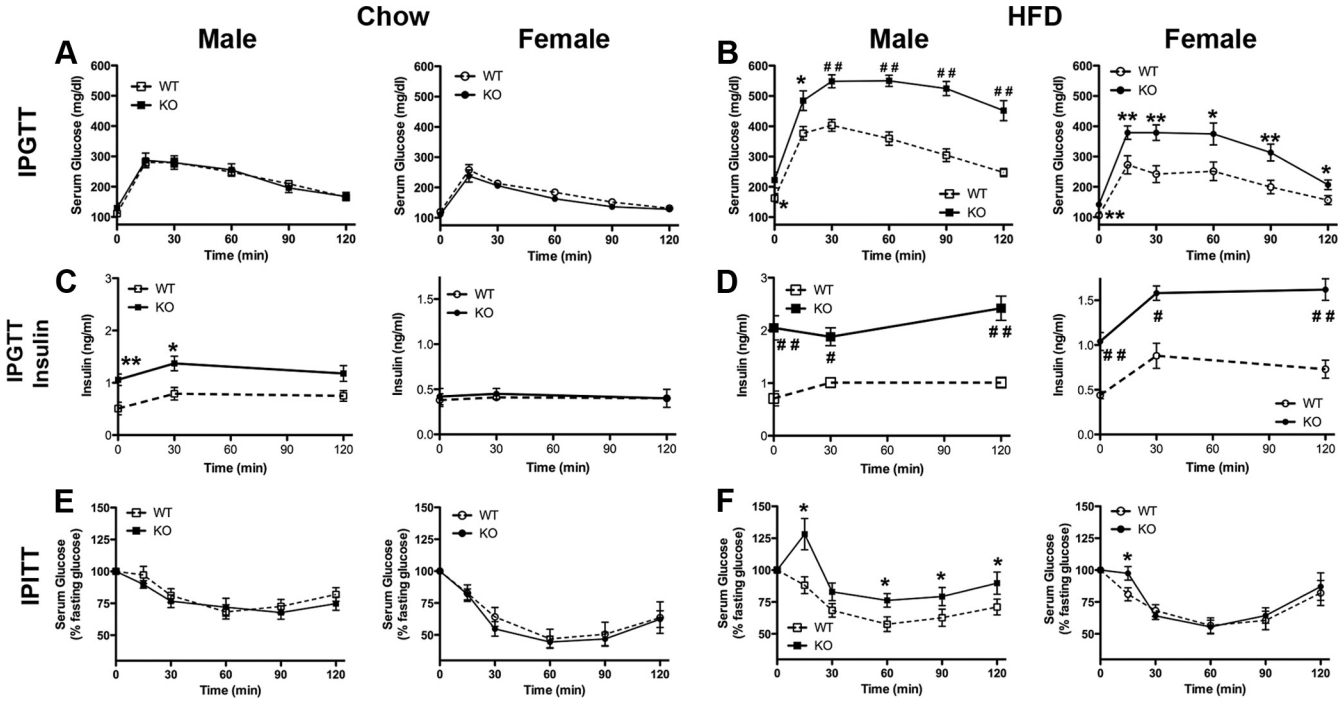

FIG. 3. Sex-specific insulin resistance in TIMP-2 KO mice. Although chow-fed TIMP-2 KO mice displayed normal glucose tolerance (A), HFD-fed TIMP-2 KO mice of both sexes were glucose intolerant (B). Male TIMP-2 KO mice were more intolerant than female KO mice, because many readings exceeded the glucometer's 600 mg/dl maximum. C, Fasting and glucose-stimulated insulin levels were increased in chow-fed male, but not female, TIMP-2 KO mice. D, Fasting and glucose-stimulated insulin levels were increased in HFD-fed TIMP-2 KO mice of both sexes. Although chow-fed TIMP-2 KO mice displayed normal insulin responsiveness (E), only male HFD-fed TIMP-2 KO mice were insulin resistant (F). n = 4–8; *, $P < 0.05$; **, $P \leq 0.01$; #, $P \leq 0.001$; ##, $P < 0.0001$.

spectively (Fig. 3). There was no significant difference in fasting glucose, and both genotypes and sexes of chow-fed mice displayed comparable responses to glucose administration (Fig. 3A). Although chow-fed male TIMP-2 KO mice did not exhibit insulin resistance (Fig. 3E) or enhanced β-cell mass (Fig. 4A), their elevated postprandial glucose levels (Fig. 2B) and fasting insulin levels (Fig. 3C) suggest a mild β-cell defect or a defect in hepatic glucose production but not severe enough to induce hepatic insulin resistance. These data also suggest that these mice may be in a progressive prediabetic phase. In contrast, HFD-fed TIMP-2 KO mice had increased fasting glucose levels and showed impaired glucose tolerance that was more pronounced in male than female TIMP-2 KO mice (Fig. 3B). In fact, the glucose values for male HFD-fed TIMP-2 KO mice are underestimations, because many readings exceeded the glucometer maximum of 600 mg/dl. Although displaying normal glucose tolerance, chow-fed male TIMP-2 KO mice exhibited increased fasting insulin levels that remained elevated during the IPGTT (Fig. 3C). However, values were at least 2-fold lower than male HFD-fed TIMP-2 KO mice (Fig. 3D). Both fasting and glucose-stimulated insulin levels were increased in HFD-fed TIMP-2 KO mice of both sexes, possibly due to hepatic insulin resistance and a compensatory increase in insulin secretion (Fig. 3D). Although chow-fed WT and TIMP-2 KO mice displayed comparable insulin sensitivity (Fig. 3E), male HFD-fed TIMP-2 KO mice were insulin resistant (Fig. 3F). The increased glucose levels in male and female TIMP-2 KO mice at 15 min after injection is likely due to stress-mediated glucose release, because TIMP-2 KO mice exhibit increased anxiety (28). Although female HFD-fed TIMP-2 KO mice were obese and moderately glucose intolerant, their peripheral tissues were insulin sensitive, suggesting a diet-dependent, male-specific defect in glucose utilization and insulin responsiveness.

Enhanced β-cell mass and proliferation in male HFD-fed TIMP-2 KO mice

Pancreatic β-cell mass dynamically changes to maintain euglycemia in response to altered metabolic demand and can be influenced by β-cell size (hypertrophy or atrophy), β-cell renewal (proliferation and differentiation), and β-cell death (29). Because only male TIMP-2 KO mice displayed insulin resistance (Fig. 3F), pancreatic physiology was only examined in male mice (Fig. 4). β-Cell mass was significantly increased in HFD-fed TIMP-2 KO mice (Fig. 4A). Nonetheless, relative islet size and number in both chow- and HFD-fed WT and TIMP-2 KO mice were comparable ($P = 0.32$) (data not shown), suggesting that the mass augmentation was not due to islet hypertrophy or enhanced neogenesis. In contrast, β-cell proliferation was

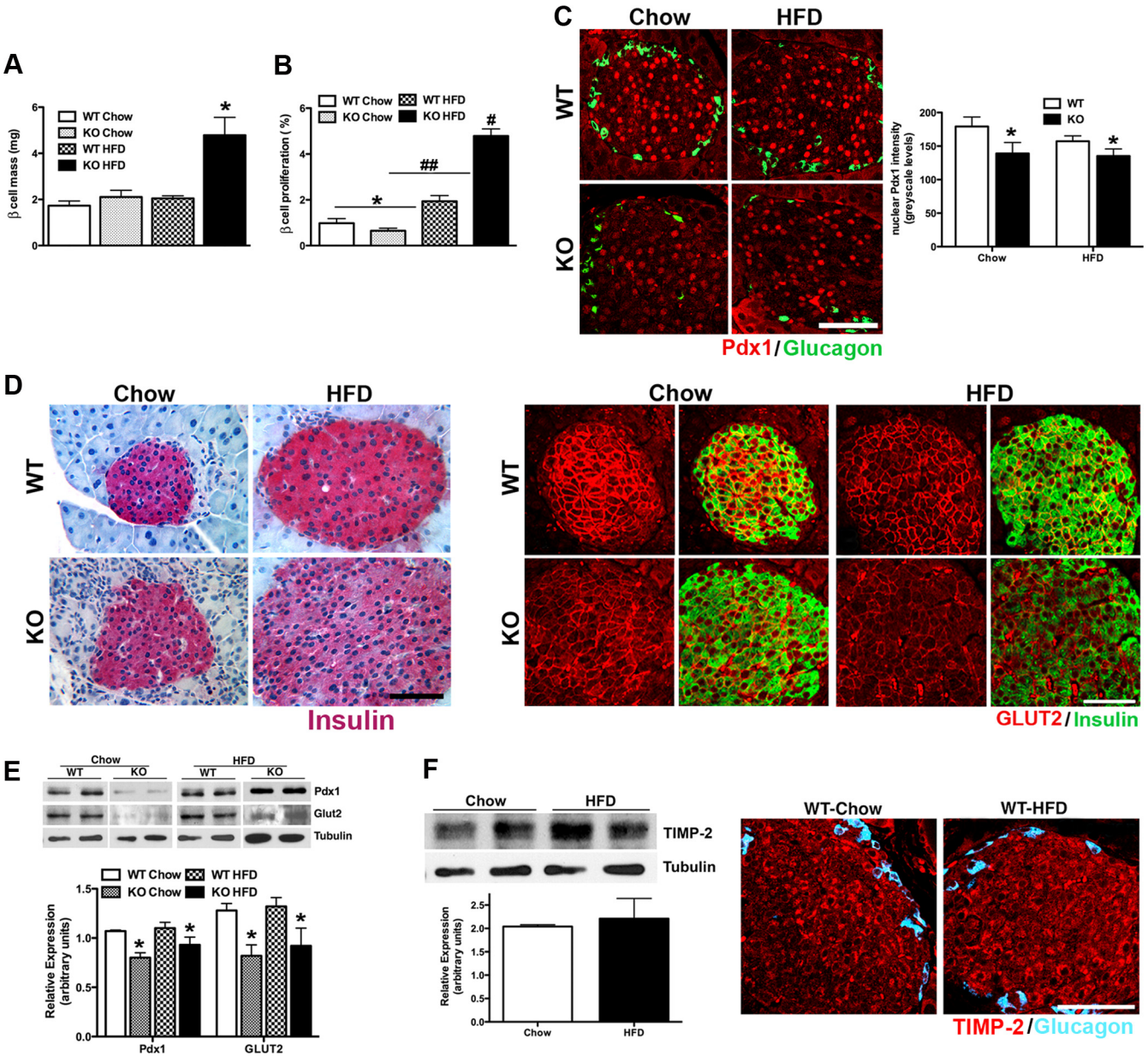

FIG. 4. β-Cell compensation to diet-induced obesity in TIMP-2 KO mice. A, β-Cell mass was increased in male TIMP-2 KO, but not WT, HFD-fed mice (genotype, $P = 0.003$; diet, $P = 0.004$). B, β-Cell proliferation was unaltered in chow-fed TIMP-2 KO mice but increased in HFD-fed TIMP-2 KO mice to a greater extent than HFD-fed WT mice (diet, $P < 0.0001$; genotype, $P = 0.0001$). C, Male TIMP-2 KO islets *in vivo* displayed decreased Pdx1 expression. D, Both insulin and GLUT2 expression were decreased in TIMP-2 KO islets *in vivo*. E, Western blot analysis of isolated islets confirmed decreased Pdx1 and GLUT2 expression observed *in vivo*. F, HFD had no effect on TIMP-2 expression in isolated islets (Western blotting) or islets *in vivo* (immunofluorescence). *Scale bars*, 50 μm. n = 4; *, $P < 0.05$; #, $P < 0.001$; ##, $P < 0.0001$.

significantly affected by diet and genotype (Fig. 4B) and most likely contributed to enhanced β-cell mass (Fig. 4A). Expression of the β-cell transcriptional regulator Pdx1 was decreased in TIMP-2 KO males (Fig. 4, C and E). Insulin and the glucose transporter GLUT2 were similarly decreased (Fig. 4, D and E). Taken together, these data suggest reduced insulin content and β-cell function in HFD-fed TIMP-2 KO mice. However, given that TIMP-2 expression was unaffected by HFD in isolated WT islets or islets *in vivo* (Fig. 4F), it suggests that the β-cell alterations observed in TIMP-2 KO mice may be secondary to diet-induced lipotoxicity and not directly to TIMP-2 deficiency.

Expression of inflammatory markers is enhanced in male TIMP-2 KO adipose tissue

Next, the effect of TIMP-2 deficiency on adipose tissue was examined (Fig. 5). In contrast to the pancreas, HFD consumption induced a significant reduction in TIMP-2 expression in adipose tissue but only in male WT mice (Fig. 5A). Furthermore, TIMP-2 displayed distinct sex-specific expression in adipose stores (*i.e.* most abundant in sc ad-

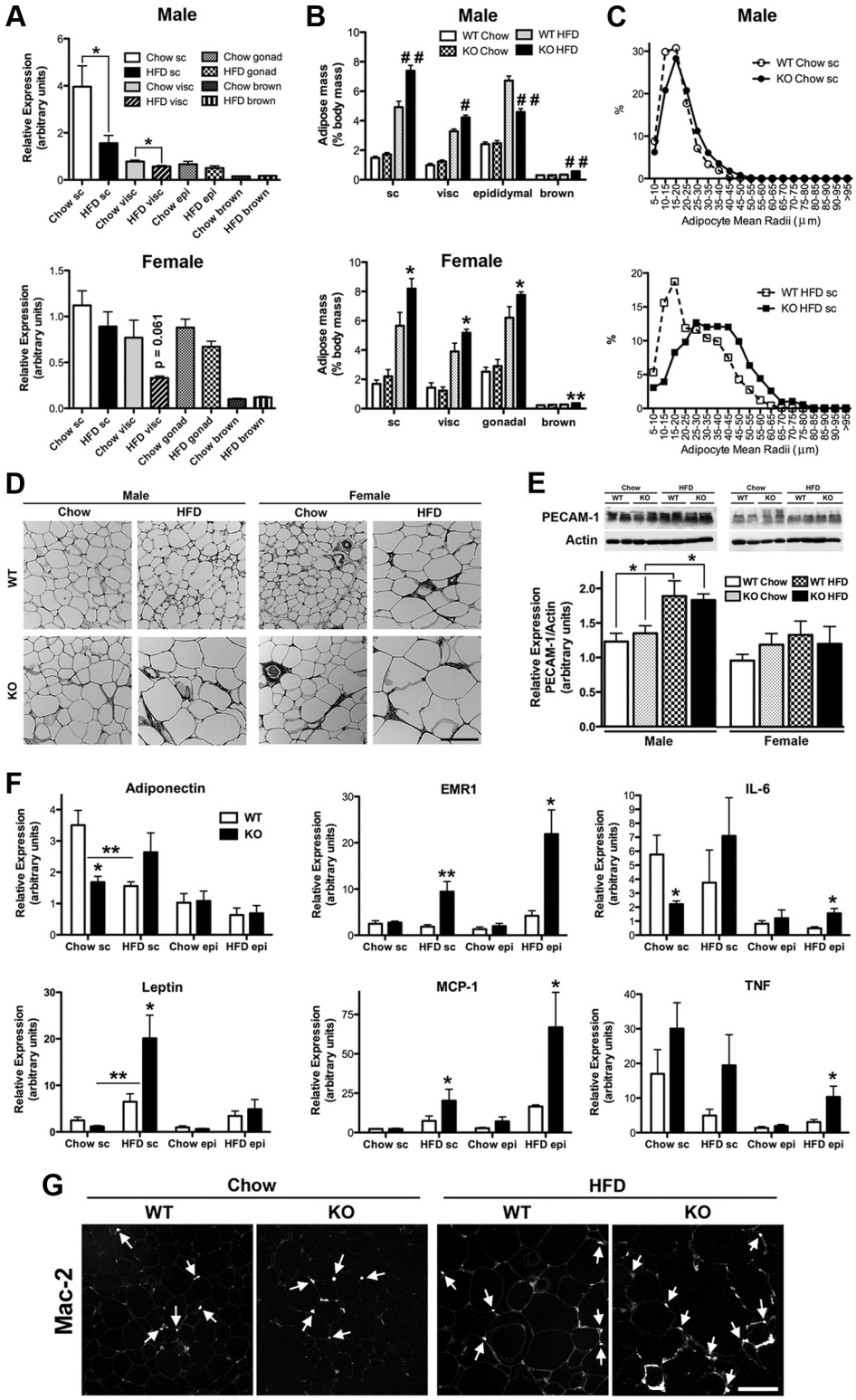

FIG. 5. Increased inflammation in male TIMP-2 KO adipose tissue. A, TIMP-2 mRNA expression was significantly decreased in response to HFD within male WT sc and visceral (visc) but not epididymal (epi) or brown adipose tissue. B, Although increased adipose tissue mass was not detected in chow-fed TIMP-2 KO mice (M, $P = 0.44$; F, $P = 0.53$) with the technique used (*i.e.* dissected wet tissue weight), adipose mass was significantly increased in HFD-fed TIMP-2 KO mice. C, In contrast to the pancreas, increased adipose mass was associated with adipocyte hypertrophy in both chow- and HFD-fed male TIMP-2 KO mice. D, Subcutaneous adipose tissue histology revealed by hematoxylin and eosin staining. *Scale bar*, 100 μm. E, HFD increased vascularization (as revealed by Western blot analysis of PECAM-1 expression) comparably in WT and TIMP-2 KO male sc adipose tissue but did not alter vascularization in female mice. F, Quantitative real-time PCR revealed increased transcriptional adipokine (adiponectin and leptin), macrophage (EMR1 and MCP-1), and proinflammatory cytokine (IL-6 and TNFα) expression, suggesting increased inflammation in male HFD-fed TIMP-2 KO adipose tissue. G, HFD induced macrophage infiltration (as revealed by an increased number of Mac-2 immunoreactive cells) to a greater extent in male TIMP-2 KO than WT sc adipose tissue. *Scale bar*, 100 μm. n = 8 (B), n = 4 (all others); *, $P < 0.05$; **, $P \leq 0.01$; #, $P \leq 0.001$; ##, $P < 0.0001$.

ipose tissue in males with comparable expression in all white adipose depots in females). Although body mass was increased in chow-fed TIMP-2 KO mice (Fig. 1A), when adipose tissue was meticulously removed and weighed, no difference in percentage body fat was present in chow-fed mice (Fig. 5B). In contrast, adipose tissue mass was significantly increased in HFD-fed TIMP-2 KO mice of both sexes. Moreover, gonadal adipose mass was increased in females, and it was decreased in males, suggesting a redistribution of adipose depots. In contrast to pancreatic β-cells, adipose mass augmentation was associated with hypertrophic sc adipocytes in both chow-fed (WT, 17.79 ± 6.73 μm; KO, 20.46 ± 8.31 μm; $P < 0.0001$) and HFD-fed (WT, 26.49 ± 12.63 μm; KO, 35.57 ± 14.72 μm; $P < 0.0001$) TIMP-2 KO mice (Fig. 5, C and D). Given that adipogenesis is tightly associated with angiogenesis (30) and TIMP-2 exerts antiangiogenic effects (31), we examined whether TIMP-2 KO mice exhibited increased vascularization (Fig. 5E). HFD increased vascularization (as revealed by CD31/PECAM-1 expression) in male, but not female, mice, but no genotype difference was observed. Finally, the transcriptional regulation of several adipose-derived bioactive molecules was examined (Fig. 5F). Although adipokine (*e.g.* adiponectin and leptin) expression was only regulated in sc adipose tissue, expression of macrophage markers (*e.g.* EMR1 and MCP-1) and proinflammatory cytokines (*e.g.* IL-6 and TNFα) were upregulated in both sc and epididymal adipose tissue of HFD-fed TIMP-2 KO males. Immunohistochemical examination revealed increased macrophage infiltration in HFD-fed male sc adipose tissue, which was greater in TIMP-2 KO mice (Fig. 5G). Thus, these data support an enhanced inflammatory state in adipose tissue of HFD-fed TIMP-2 KO males.

Contribution of membrane type 1 (MT1)-MMP-mediated collagenolysis to the TIMP-2 KO hyperlipotrophic phenotype

Inasmuch as numerous MMPs are transcriptionally regulated by inflammatory cytokines (32), MT1-MMP (MMP-14) expression is increased in TIMP-2 KO heart (33), lung (22), and myoblasts (34), and MT1-MMP deficient mice (13) and adipocytes (12) display a lipodystrophic phenotype, we examined whether, by extension, increased MT1-MMP expression in adipose tissue could contribute to the hyperlipotrophic TIMP-2 KO phenotype (Fig. 6). MT1-MMP expression (*i.e.* pro-MT1-MMP) and activity (*i.e.* active MT1-MMP) were comparable in the sc

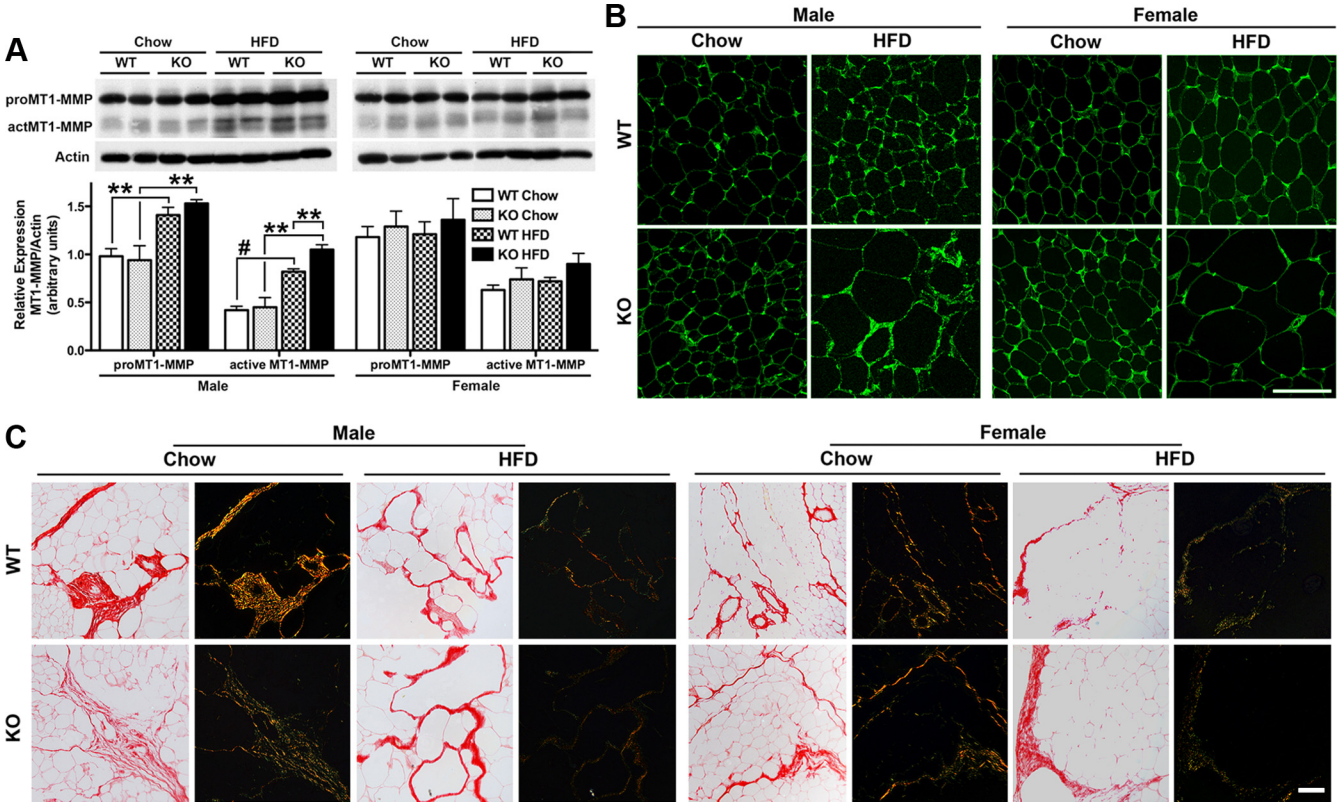

FIG. 6. Sex-specific increased collagenolysis in response to diet-induced obesity. A, HFD induced increased pro-MT1-MMP expression and MT1-MMP activity in male, but not female, sc adipose tissue. MT1-MMP activity was increased a greater extent in TIMP-2 KO mice. B, MT1-MMP immunoreactivity in sc adipose tissue. C, Brightfield and polarization microscopy photomicrographs of Sirius Red staining demonstrating decreased connective tissue and pericellular adipocyte collagen integrity in HFD-fed male sc tissue, consistent with increased MT1-MMP activity. *Scale bars*, 100 μm. n = 4; **, $P \leq 0.01$; #, $P \leq 0.001$.

adipose tissue of chow-fed WT and TIMP-2 KO mice of both sexes (Fig. 6, A and B). Interestingly, HFD increased MT1-MMP expression and activity in male, but not female, mice (Fig. 6, A and B). More strikingly, MT1-MMP activity was increased a greater extent in TIMP-2 KO mice (Fig. 6A) and was associated with decreased Sirius Red staining (Fig. 6C), indicative of increased collagenolysis. Collectively, our data support a contribution of MT1-MMP and its primary inhibitor, TIMP-2, to increased collagen turnover during diet-induced adipogenesis.

Discussion

This study is the first to report an MMP- or TIMP-deficient mouse model in which both sexes develop obesity even when fed a standard chow diet. Although chow-fed TIMP-2 KO mice are obese, they are spared the adverse metabolic consequences. Inasmuch as male, but not female, HFD-fed TIMP-2 KO mice develop insulin resistance, TIMP-2 expression is down-regulated and MMP-14 activity is increased in male, but not female, adipose tissue. This suggests that dysregulated MMP-14/TIMP-2 expression may contribute to the observed sex-specific diet-induced insulin resistance.

The most parsimonious explanation for the metabolic phenotype observed in TIMP-2 KO mice is rampant MMP-mediated proteolysis. MMP levels are elevated in both human T2DM (35) and murine diabetes models (36), supporting this hypothesis. However, MMPs are also increased in obesity (16) and cardiovascular disease (37), two common diabetes comorbidities; thus, making it difficult to discern the individual *vs.* collective contributions of MMPs. Nonetheless, increased TNFα-converting enzyme (TACE, ADAM17)-mediated proteolysis of the TNFα and IL-6 receptor has recently been implicated in the pathogenesis of insulin resistance (38, 39), and TNFα and IL-6 expression was increased in HFD-fed TIMP-2 KO adipose tissue. Cytokine-mediated MMP activation disrupts endothelial cell-cell adhesion, permitting macrophage infiltration and further enhancement of MMP activation (40). The finding that increased EMR1 and MCP-1 expression (Fig. 5F) was associated with increased macrophage infiltration in HFD-fed TIMP-2 KO adipose tissue (Fig. 5G) supports this assertion. MMPs could also contribute to insulin resistance and obesity via cleavage of insulin (41) or IGF binding proteins (42). In the presence of increased IGF binding protein proteolysis, insulin/IGF-I anabolic bioactivity would be increased. The adiposity in TIMP-2 KO mice could result from feedback of elevated IGF-1 to the hypothalamus and pituitary gland to decrease growth hormone levels, leading to lipogenesis and triacylglycerol accumulation, which would require enhanced pericellular adipocyte ECM remodeling. MMP-14-mediated collagenolysis plays a critical role in the development of adipocytes (12) and an obesogenic phenotype (10). Furthermore, a HFD increases MMP-14-mediated collagen turnover, and human MMP-14 gene polymorphisms near the catalytic domain correlate with sexually dimorphic obese and diabetic phenotypes (10). Interestingly, one MMP-14 haplotype was consistently associated with increased fasting blood glucose and insulin resistance in males, supporting a potential link between MMP-14 and diabetes in males. That MMP-14 activity was increased in male HFD-fed TIMP-2 KO adipose tissue to a greater extent than WT adipose tissue supports a potential contribution of MMP-14 to the TIMP-2 KO sexually dimorphic male-specific insulin resistance. Dysregulated MMP-mediated ECM proteolysis may contribute to other aspects of the TIMP-2 KO metabolic phenotype. For example, MMP activity is increased in the TIMP-2 KO arcuate nucleus of the hypothalamus (43), a key brain region regulating food intake and energy homeostasis. Adipose-derived leptin promotes anorexigenic (*i.e.* satiety promoting) and inhibits orexigenic neuropeptide expression within the arcuate nucleus via activation of Jak2/STAT3 signaling. TIMP-2 KO mice did not exhibit altered expression of anorexigenic or orexigenic neuropeptides but displayed attenuated leptin-mediated STAT3 activation and anorectic responses in food consumption and weight loss, indicative of leptin resistance (43). Although MMPs play a well-accepted role in cerebral cortical synaptic plasticity (44, 45), the potential contribution of MMPs to hypothalamic plasticity in central control of energy homeostasis is an unexplored area. Because administration of galardin, a broad-spectrum hydroxamate-based MMP inhibitor, to HFD-fed WT mice resulted in significant reduction of adipose tissue mass (46), but Ro28–2653, a more selective MMP-2, MMP-9, and MMP-14 inhibitor, did not significantly affect adipose tissue development (47), it demonstrates the need to identify the repertoire of MMPs dysregulated in obesity if MMP inhibition is to be used therapeutically.

If increased MMP expression alone were the basis for the TIMP-2 KO metabolic phenotype, then all TIMP KO mice might be expected to exhibit similar phenotypes. Although plasma TIMP-1 predicts human obesity (48), TIMP-1 does not affect adipogenesis (49, 50) and chow-fed male TIMP-1 KO mice are not obese (19). Similarly, chow-fed TIMP-3 KO mice do not exhibit insulin resistance or obesity (21). Unlike other TIMPs, TIMP-2 also plays a role in pro-MMP activation (*i.e.* MMP-14-mediated pro-MMP-2 activation). Thus, increased adipose MMP-14 expression and activity (Fig. 6A) could simply represent a compensatory mechanism to maintain pro-

MMP-2 activation in the context of decreased TIMP-2 upon high-fat feeding (Fig. 5A), similar to the up-regulation of MMP-14 observed in TIMP-2 KO tissues under basal conditions (22, 33, 34). The lack of increased MMP-14 activity in chow-fed TIMP-2 KO adipose tissue suggests that a simple compensatory mechanism is unlikely. Alternatively, MMP-14 up-regulation may be dependent on the relative abundance of pro-MMP-2 within a particular tissue. For example, net proteolysis is decreased in TIMP-2 KO muscle (51), which expresses abundant MMP-2, but is increased in TIMP-2 KO hypothalamus (43), which possesses less MMP-2. Although adult adipose tissue expresses abundant MMP-2 (52), obesity in TIMP-2 KO mice is probably not due to MMP-2 deficiency, because MMP-2 KO mice are protected from HFD-induced obesity (11).

TIMP-2 also exerts diverse pleiotropic MMP-independent roles mediated via integrin signaling. Adipogenesis and angiogenesis are tightly associated (30) in that treatment with antiangiogenic agents results in a dose-dependent, reversible weight reduction and adipose tissue loss (53). Because TIMP-2 exerts MMP-independent antiangiogenic activities (18) and most MMPs/TIMPs are enriched in stromal-vascular cells relative to adipocytes (54), one would expect increased angiogenesis in TIMP-2 KO adipose tissue; nonetheless, PECAM-1 expression was not increased (Fig. 5E). Similarly, TIMP-2 also exerts antiproliferative effects (55), but β-cell proliferation was unaltered in chow-fed TIMP-2 KO mice. Although β-cell proliferation was increased in HFD-fed TIMP-2 KO mice (Fig. 4B), HFD did not alter TIMP-2 expression in WT islets (Fig. 4F); thus, supporting our assertion that β-cells are adapting to increased adiposity. β-Cells initially compensate for obesity and associated insulin resistance by increasing β-cell mass, insulin content, and secretion but eventually become dysfunctional, because they cannot meet the body's demand for insulin (56). The ensuing β-cell exhaustion and insulin degranulation is associated with hyperglycemia and, ultimately, diabetes. The development of diabetes due to insufficient compensation has been observed in several animal models, including the Zucker diabetic fatty rat, and human obese patients (57). Although male HFD-fed TIMP-2 KO mice are compensating in response to insulin resistance, as demonstrated by enhanced β-cell mass (Fig. 4A) and hyperinsulinemia (Fig. 2C), they are likely on the verge of β-cell failure as evidenced by elevated fed and fasting blood glucose levels (Fig. 2) and diminished insulin immunostaining, suggesting degranulation (Fig. 4D). Their severe glucose intolerance (Fig. 3B) and decreased levels of GLUT2 (Fig. 4, D and E), a β-cell glucose sensor component, suggest they may also suffer from impaired β-cell glucose sensitivity. Although only male HFD-fed TIMP-2 KO mice develop insulin resistance, female HFD-fed TIMP-2 KO mice are also glucose intolerant and hyperinsulinemic. Sex steroid hormones could contribute to the observed sexually dimorphic insulin resistance. Female rodents are, in general, protected from diabetes compared with males due, in part, to the multifactorial beneficial actions of β-cell estrogen receptors and the oxidative stress-promoting actions of β-cell androgen receptors (58). In addition, β-cell estrogen receptor-α may also promote growth and new β-cell development (59, 60). In contrast, there is a strong curvilinear association between obesity and diabetes risk in humans such that there is no sex difference in the prevalence of obesity or diabetes (61). Alternatively, the failure of female HFD-fed TIMP-2 KO mice to develop insulin resistance may be due to the relatively low endogenous TIMP-2 expression in female HFD-fed WT visceral adipose depots, compared with the abundant TIMP-2 expression in male HFD-fed WT depots (Fig. 5A).

Finally, the contribution of TIMP-2 within liver and skeletal muscle to insulin resistance and obesity, as well as central defects underlying the regulation of caloric intake, must be taken into account. Chronically elevated plasma free fatty acids and proinflammatory cytokines are known to have pathophysiological consequences in liver (*i.e.* enhanced gluconeogenesis) (62), muscle (*i.e.* reduced glucose uptake through decreased GLUT4 translocation) (63), and β-cells (*i.e.* enhanced oxidative stress) (64). Although our data support an effect of free fatty acids and cytokines in liver and β-cells, we cannot, at present, exclude a contribution of skeletal muscle to the TIMP-2 KO metabolic phenotype. TIMP-2 KO mice display motor deficits (65) and decreased mass of the extensor digitorum longus, a predominantly fast-twitch muscle (51), perhaps leading to weakness and increased adiposity simply due to a more sedentary lifestyle. If more oxidative slow-twitch muscle (*e.g.* soleus) were also lost in TIMP-2 KO mice, this could more directly promote insulin resistance, because oxidative type-1 muscle plays a key role in glucose disposal [*i.e.* handles 75–95% of all insulin-mediated glucose usage (66)]. We propose that hepatic insulin resistance prevails in HFD-fed TIMP-2 KO mice, because studies have shown that β-cell hyperplasia occurs only in response to hepatic, but not muscle, insulin resistance (67–69). To fully address whether glucose intolerance and insulin resistance are related to hepatic glucose production or to peripheral uptake of glucose, hyperinsulinemic euglycemic clamp studies or immunoblotting for Akt levels in liver, muscle, or adipose tissue would be required. Because muscle-specific depletion of β1 integrin is associated with insulin resistance (70) and TIMP-2 regulates β1 integrin expression in muscle (34, 51), it is intriguing to speculate that a

sex-specific reduction of β1 integrin expression may underlie the insulin resistance in male TIMP-2 KO mice. Unfortunately, the study by Zong *et al.* (70) only examined male mice, and no mention was made of increased adiposity. However, because β1 integrins also contribute to β-cell differentiation (71), future studies are warranted to examine sex-specific β1 integrin expression in both muscle and β-cells.

Acknowledgments

We thank Dr. Paul D. Soloway (Division of Nutritional Sciences, Cornell University, Ithaca, New York) for graciously providing TIMP-2 KO mice and Marilyn Wadsworth of the University of Vermont College of Medicine Microscopy Imaging Center for providing Mac-2 antibody, performing pico-Sirius Red staining, and assisting with polarization microscopy. The Pdx1 monoclonal antibody developed by O. D. Madsen was obtained from the Developmental Studies Hybridoma Bank developed under the auspices of the National Institute of Child Health and Human Development and maintained by Department of Biology, The University of Iowa (Iowa City, Iowa).

Address all correspondence and requests for reprints to: Dr. Diane M. Jaworski, Department of Anatomy and Neurobiology, University of Vermont College of Medicine, 149 Beaumont Avenue, HSRF 418, Burlington, Vermont 05405. E-mail: diane.jaworski@uvm.edu.

This work was supported by National Institute of Neurological Disorders and Stroke/National Center for Research Resources (NCRR) Grant NS045225 (to D.M.J.), Grant DK068329 (to T.L.J.) and by the Juvenile Diabetes Research Foundation (M.P.). The equipment provided by the Neuroscience COBRE Molecular Core Facility was supported by the National Institutes of Health (NIH) NCRR Grant P20 RR016435, and the Vermont Cancer Center DNA Facility was supported by NIH Grant P30 CA22435.

Disclosure Summary: The authors have nothing to disclose.

References

1. **Flegal KM, Carroll MD, Ogden CL, Curtin LR** 2010 Prevalence and trends in obesity among US adults, 1999–2008. JAMA 303:235–241
2. **Ogden CL, Carroll MD, Curtin LR, Lamb MM, Flegal KM** 2010 Prevalence of high body mass index in US children and adolescents, 2007–2008. JAMA 303:242–249
3. **Goodpaster BH, Krishnaswami S, Resnick H, Kelley DE, Haggerty C, Harris TB, Schwartz AV, Kritchevsky S, Newman AB** 2003 Association between regional adipose tissue distribution and both type 2 diabetes and impaired glucose tolerance in elderly men and women. Diabetes Care 26:372–379
4. **Gallagher D, Kuznia P, Heshka S, Albu J, Heymsfield SB, Goodpaster B, Visser M, Harris TB** 2005 Adipose tissue in muscle: a novel depot similar in size to visceral adipose tissue. Am J Clin Nutr 81:903–910
5. **Yki-Järvinen H** 2005 Fat in the liver and insulin resistance. Ann Med 37:347–356
6. **Rodríguez D, Morrison CJ, Overall CM** 2010 Matrix metalloproteinases: what do they not do? New substrates and biological roles identified by murine models and proteomics. Biochim Biophys Acta 1803:39–54
7. **Pendás AM, Folgueras AR, Llano E, Caterina J, Frerard F, Rodríguez F, Astudillo A, Noël A, Birkedal-Hansen H, López-Otín C** 2004 Diet-induced obesity and reduced skin cancer susceptibility in matrix metalloproteinase 19-deficient mice. Mol Cell Biol 24:5304–5313
8. **Maquoi E, Demeulemeester D, Vörös G, Collen D, Lijnen HR** 2003 Enhanced nutritionally induced adipose tissue development in mice with stromelysin-1 gene inactivation. Thromb Haemost 89:696–704
9. **Lijnen HR, Van HB, Frederix L, Rio MC, Collen D** 2002 Adipocyte hypertrophy in stromelysin-3 deficient mice with nutritionally induced obesity. Thromb Haemost 87:530–535
10. **Chun TH, Inoue M, Morisaki H, Yamanaka I, Miyamoto Y, Okamura T, Sato-Kusubata K, Weiss SJ** 2010 Genetic link between obesity and MMP14-dependent adipogenic collagen turnover. Diabetes 59:2484–2494
11. **Van Hul M, Lijnen HR** 2008 A functional role of gelatinase A in the development of nutritionally induced obesity in mice. J Thromb Haemost 6:1198–1206
12. **Chun TH, Hotary KB, Sabeh F, Saltiel AR, Allen ED, Weiss SJ** 2006 A pericellular collagenase directs the 3-dimensional development of white adipose tissue. Cell 125:577–591
13. **Holmbeck K, Bianco P, Caterina J, Yamada S, Kromer M, Kuznetsov SA, Mankani M, Robey PG, Poole AR, Pidoux I, Ward JM, Birkedal-Hansen H** 1999 MT1-MMP-deficient mice develop dwarfism, osteopenia, arthritis, and connective tissue disease due to inadequate collagen turnover. Cell 99:81–92
14. **Van Hul M, Piccard H, Lijnen HR** 2010 Gelatinase B (MMP-9) deficiency does not affect murine adipose tissue development. Thromb Haemost 104:165–171
15. **Lijnen HR, Van Hoef B, Rodriguez JA, Paramo JA** 2009 Stromelysin-2 (MMP-10) deficiency does not affect adipose tissue formation in a mouse model of nutritionally induced obesity. Biochem Biophys Res Commun 389:378–381
16. **Derosa G, Ferrari I, D'Angelo A, Tinelli C, Salvadeo SA, Ciccarelli L, Piccinni MN, Gravina A, Ramondetti F, Maffioli P, Cicero AF** 2008 Matrix metalloproteinase-2 and -9 levels in obese patients. Endothelium 15:219–224
17. **Brew K, Nagase H** 2010 The tissue inhibitors of metalloproteinases (TIMPs): an ancient family with structural and functional diversity. Biochim Biophys Acta 1803:55–71
18. **Stetler-Stevenson WG** 2008 Tissue inhibitors of metalloproteinases in cell signaling: metalloproteinase-independent biological activities. Sci Signal 1:re6
19. **Lijnen HR, Demeulemeester D, Van Hoef B, Collen D, Maquoi E** 2003 Deficiency of tissue inhibitor of matrix metalloproteinase-1 (TIMP-1) impairs nutritionally induced obesity in mice. Thromb Haemost 89:249–255
20. **Gerin I, Louis GW, Zhang X, Prestwich TC, Kumar TR, Myers Jr MG, Macdougald OA, Nothnick WB** 2009 Hyperphagia and obesity in female mice lacking tissue inhibitor of metalloproteinase-1. Endocrinology 150:1697–1704
21. **Menghini R, Menini S, Amoruso R, Fiorentino L, Casagrande V, Marzano V, Tornei F, Bertucci P, Iacobini C, Serino M, Porzio O, Hribal ML, Folli F, Khokha R, Urbani A, Lauro R, Pugliese G, Federici M** 2009 Tissue inhibitor of metalloproteinase 3 deficiency causes hepatic steatosis and adipose tissue inflammation in mice. Gastroenterology 136:663–672.
22. **Wang Z, Juttermann R, Soloway PD** 2000 TIMP-2 is required for efficient activation of proMMP-2 *in vivo*. J Biol Chem 275:26411–26415
23. **Jetton TL, Lausier J, LaRock K, Trotman WE, Larmie B, Habibovic**

A, Peshavaria M, Leahy JL 2005 Mechanisms of compensatory β-cell growth in insulin-resistant rats: roles of Akt kinase. Diabetes 54:2294–2304
24. **Peshavaria M, Larmie BL, Lausier J, Satish B, Habibovic A, Roskens V, Larock K, Everill B, Leahy JL, Jetton TL** 2006 Regulation of pancreatic β-cell regeneration in the normoglycemic 60% partial-pancreatectomy mouse. Diabetes 55:3289–3298
25. **Lluri G, Jaworski DM** 2005 Regulation of TIMP-2, MT1-MMP, and MMP-2 expression during C2C12 differentiation. Muscle Nerve 32:492–499
26. **Junqueira LC, Cossermelli W, Brentani R** 1978 Differential staining of collagens type I, II and III by sirius red and polarization microscopy. Arch Histol Jpn 41:267–274
27. **Levin BE** 2006 Metabolic imprinting: critical impact of the perinatal environment on the regulation of energy homeostasis. Philos Trans R Soc Lond B Biol Sci 361:1107–1121
28. **Jaworski DM, Boone J, Caterina J, Soloway P, Falls WA** 2005 Prepulse inhibition and fear-potentiated startle are altered in tissue inhibitor of metalloproteinase-2 (TIMP-2) knockout mice. Brain Res 1051:81–89
29. **Ballian N, Hu M, Liu SH, Brunicardi FC** 2007 Proliferation, hyperplasia, neogenesis, and neoplasia in the islets of Langerhans. Pancreas 35:199–206
30. **Christiaens V, Lijnen HR** 2010 Angiogenesis and development of adipose tissue. Mol Cell Endocrinol 318:2–9
31. **Stetler-Stevenson WG, Seo DW** 2005 TIMP-2: an endogenous inhibitor of angiogenesis. Trends Mol Med 11:97–103
32. **Clark IM, Swingler TE, Sampieri CL, Edwards DR** 2008 The regulation of matrix metalloproteinases and their inhibitors. Int J Biochem Cell Biol 40:1362–1378
33. **Kandalam V, Basu R, Abraham T, Wang X, Soloway PD, Jaworski DM, Oudit GY, Kassiri Z** 2010 TIMP2 deficiency accelerates adverse post-myocardial infarction remodeling because of enhanced MT1-MMP activity despite lack of MMP2 activation. Circ Res 106:796–808
34. **Lluri G, Langlois GD, Soloway PD, Jaworski DM** 2008 Tissue inhibitor of metalloproteinase-2 (TIMP-2) regulates myogenesis and β1 integrin expression in vitro. Exp Cell Res 314:11–24
35. **Derosa G, D'Angelo A, Tinelli C, Devangelio E, Consoli A, Miccoli R, Penno G, Del Prato S, Paniga S, Cicero AF** 2007 Evaluation of metalloproteinase 2 and 9 levels and their inhibitors in diabetic and healthy subjects. Diabetes Metab 33:129–134
36. **Zhou YP, Madjidi A, Wilson ME, Nothhelfer DA, Johnson JH, Palma JF, Schweitzer A, Burant C, Blume JE, Johnson JD** 2005 Matrix metalloproteinases contribute to insulin insufficiency in Zucker diabetic fatty rats. Diabetes 54:2612–2619
37. **Derosa G, D'Angelo A, Scalise F, Avanzini MA, Tinelli C, Peros E, Fogari E, Cicero AF** 2007 Comparison between metalloproteinases-2 and -9 in healthy subjects, diabetics, and subjects with acute coronary syndrome. Heart Vessels 22:361–370
38. **Fiorentino L, Vivanti A, Cavalera M, Marzano V, Ronci M, Fabrizi M, Menini S, Pugliese G, Menghini R, Khokha R, Lauro R, Urbani A, Federici M** 2010 Increased tumor necrosis factor a-converting enzyme activity induces insulin resistance and hepatosteatosis in mice. Hepatology 51:103–110
39. **Monroy A, Kamath S, Chavez AO, Centonze VE, Veerasamy M, Barrentine A, Wewer JJ, Coletta DK, Jenkinson C, Jhingan RM, Smokler D, Reyna S, Musi N, Khokka R, Federici M, Tripathy D, DeFronzo RA, Folli F** 2009 Impaired regulation of the TNF-α converting enzyme/tissue inhibitor of metalloproteinase 3 proteolytic system in skeletal muscle of obese type 2 diabetic patients: a new mechanism of insulin resistance in humans. Diabetologia 52:2169–2181
40. **Rosenberg GA** 2002 Matrix metalloproteinases in neuroinflammation. Glia 39:279–291
41. **Descamps FJ, Van den Steen PE, Martens E, Ballaux F, Geboes K, Opdenakker G** 2003 Gelatinase B is diabetogenic in acute and chronic pancreatitis by cleaving insulin. FASEB J 17:887–889
42. **Nakamura M, Miyamoto S, Maeda H, Ishii G, Hasebe T, Chiba T, Asaka M, Ochiai A** 2005 Matrix metalloproteinase-7 degrades all insulin-like growth factor binding proteins and facilitates insulin-like growth factor bioavailability. Biochem Biophys Res Commun 333:1011–1016
43. **Stradecki HM, Jaworski DM** 22 December 2010 Hyperphagia and leptin resistance in tissue inhibitor of metalloproteinase-2 (TIMP-2) deficient mice. J Neuroendocrinol 10.1111/j.1365–2826.2010.02105.x
44. **Rivera S, Khrestchatisky M, Kaczmarek L, Rosenberg GA, Jaworski DM** 2010 Metzincin proteases and their inhibitors: foes or friends in nervous system physiology? J Neurosci 30:15337–15357
45. **Ethell IM, Ethell DW** 2007 Matrix metalloproteinases in brain development and remodeling: synaptic functions and targets. J Neurosci Res 85:2813–2823
46. **Lijnen HR, Maquoi E, Hansen LB, Van Hoef B, Frederix L, Collen D** 2002 Matrix metalloproteinase inhibition impairs adipose tissue development in mice. Arterioscler Thromb Vasc Biol 22:374–379
47. **Demeulemeester D, Collen D, Lijnen HR** 2005 Effect of matrix metalloproteinase inhibition on adipose tissue development. Biochem Biophys Res Commun 329:105–110
48. **Kralisch S, Bluher M, Tonjes A, Lossner U, Paschke R, Stumvoll M, Fasshauer M** 2007 Tissue inhibitor of metalloproteinase-1 predicts adiposity in humans. Eur J Endocrinol 156:257–261
49. **Scroyen I, Cosemans L, Lijnen HR** 2009 Effect of tissue inhibitor of matrix metalloproteinases-1 on in vitro and in vivo adipocyte differentiation. Thromb Res 124:578–583
50. **Demeulemeester D, Scroyen I, Voros G, Snoeys J, De Geest B, Collen D, Lijnen HR** 2006 Overexpression of tissue inhibitor of matrix metalloproteinases-1 (TIMP-1) in mice does not affect adipogenesis or adipose tissue development. Thromb Haemost 95:1019–1024
51. **Lluri G, Langlois GD, McClellan B, Soloway PD, Jaworski DM** 2006 Tissue inhibitor of metalloproteinase-2 (TIMP-2) regulates neuromuscular junction development via a β1 integrin-mediated mechanism. J Neurobiol 66:1365–1377
52. **Bouloumié A, Sengenès C, Portolan G, Galitzky J, Lafontan M** 2001 Adipocyte produces matrix metalloproteinases 2 and 9: involvement in adipose differentiation. Diabetes 50:2080–2086
53. **Rupnick MA, Panigrahy D, Zhang CY, Dallabrida SM, Lowell BB, Langer R, Folkman MJ** 2002 Adipose tissue mass can be regulated through the vasculature. Proc Natl Acad Sci USA 99:10730–10735
54. **Maquoi E, Munaut C, Colige A, Collen D, Lijnen HR** 2002 Modulation of adipose tissue expression of murine matrix metalloproteinases and their tissue inhibitors with obesity. Diabetes 51:1093–1101
55. **Pérez-Martínez L, Jaworski DM** 2005 Tissue inhibitor of metalloproteinase-2 promotes neuronal differentiation by acting as an anti-mitogenic signal. J Neurosci 25:4917–4929
56. **Kaiser N, Yuli M, Uçkaya G, Oprescu AI, Berthault MF, Kargar C, Donath MY, Cerasi E, Ktorza A** 2005 Dynamic changes in β-cell mass and pancreatic insulin during the evolution of nutrition-dependent diabetes in *Psammomys obesus*: impact of glycemic control. Diabetes 54:138–145
57. **Kahn SE** 2001 Clinical review 135: the importance of β-cell failure in the development and progression of type 2 diabetes. J Clin Endocrinol Metab 86:4047–4058
58. **Liu S, Mauvais-Jarvis F** 2010 Minireview: estrogenic protection of β-cell failure in metabolic diseases. Endocrinology 151:859–864
59. **Yamabe N, Kang KS, Zhu BT** 2010 Beneficial effect of 17β-estradiol on hyperglycemia and islet β-cell functions in a streptozotocin-induced diabetic rat model. Toxicol Appl Pharmacol 249:76–85
60. **Liu S, Le May C, Wong WP, Ward RD, Clegg DJ, Marcelli M, Korach KS, Mauvais-Jarvis F** 2009 Importance of extranuclear estrogen receptor-α and membrane G protein-coupled estrogen receptor in pancreatic islet survival. Diabetes 58:2292–2302
61. **Kautzky-Willer A, Handisurya A** 2009 Metabolic diseases and associated complications: sex and gender matter! Eur J Clin Invest 39:631–648

62. **Boden G, Shulman GI** 2002 Free fatty acids in obesity and type 2 diabetes: defining their role in the development of insulin resistance and β-cell dysfunction. Eur J Clin Invest 32:14–23
63. **Shulman GI** 2000 Cellular mechanisms of insulin resistance. J Clin Invest 106:171–176
64. **Prentki M, Nolan CJ** 2006 Islet β cell failure in type 2 diabetes. J Clin Invest 116:1802–1812
65. **Jaworski DM, Soloway P, Caterina J, Falls WA** 2006 Tissue inhibitor of metalloproteinase-2 (TIMP-2)-deficient mice display motor deficits. J Neurobiol 66:82–94
66. **Stump CS, Henriksen EJ, Wei Y, Sowers JR** 2006 The metabolic syndrome: role of skeletal muscle metabolism. Ann Med 38:389–402
67. **Escribano O, Guillén C, Nevado C, Gómez-Hernández A, Kahn CR, Benito M** 2009 β-Cell hyperplasia induced by hepatic insulin resistance: role of a liver-pancreas endocrine axis through insulin receptor A isoform. Diabetes 58:820–828
68. **Michael MD, Kulkarni RN, Postic C, Previs SF, Shulman GI, Magnuson MA, Kahn CR** 2000 Loss of insulin signaling in hepatocytes leads to severe insulin resistance and progressive hepatic dysfunction. Mol Cell 6:87–97
69. **Brüning JC, Michael MD, Winnay JN, Hayashi T, Hörsch D, Accili D, Goodyear LJ, Kahn CR** 1998 A muscle-specific insulin receptor knockout exhibits features of the metabolic syndrome of NIDDM without altering glucose tolerance. Mol Cell 2:559–569
70. **Zong H, Bastie CC, Xu J, Fassler R, Campbell KP, Kurland IJ, Pessin JE** 2009 Insulin resistance in striated muscle-specific integrin receptor β1-deficient mice. J Biol Chem 284:4679–4688
71. **Nikolova G, Jabs N, Konstantinova I, Domogatskaya A, Tryggvason K, Sorokin L, Fässler R, Gu G, Gerber HP, Ferrara N, Melton DA, Lammert E** 2006 The vascular basement membrane: a niche for insulin gene expression and β cell proliferation. Dev Cell 10:397–405